Colorimetric *in situ* assay of membrane-bound enzyme based on lipid bilayer inhibition on ion transport

Juan Zhang[a], Defeng Li[a, b], Xiquan Yue[a], Meiling Zhang[c], Ping Liu[c]*, Genxi Li[a, d]*

[a] Center for Molecular Recognition and Biosensing, School of Life Sciences, Shanghai University, Shanghai 200444, P. R. China

[b] Shanghai Key Laboratory of Bio-Energy Crops, Shanghai University, Shanghai 200444, P. R. China

[c] Department of Oncology, the First Affiliated Hospital of Nanjing Medical University, Nanjing 210029, P. R. China

[d] State Key Laboratory of Pharmaceutical Biotechnology, Department of Biochemistry, Nanjing University, Nanjing 210093, P. R. China

* Corresponding authors. Fax: +86 25 68136043 (P. Liu); +86 25 83592510 (G. Li). E-mail addresses: liupinga28@163.com (P. Liu); genxili@nju.edu.cn (G. Li)

Methods

Preparation of AMNSs and APBA/AMNSs

The assembled magnetic nanospheres (AMNSs) were synthesized by a method reported previously [1]. Typically, $FeCl_3 \cdot 6H_2O$ (1.080 g, 4.0 mmol) and trisodium citrate (0.200 g, 0.68 mmol) were first dissolved in ethylene glycol (20 mL) under magnetic stirring. Subsequently, NaAc (1.200 g) was added. After vigorous stirring for 30 min, the mixture was transferred to a Teflon-lined stainless-steel autoclave (50 mL capacity). The autoclave was heated to 210 °C, maintained for 10 h, and then allowed to cool to room temperature. The black product was collected by magnetic separation and washed with ethanol and deionized water several times, to give AMNSs. The AMNSs were then redispersed in water and stored at room temperature for use.

For the modification of AMNSs, a routine method using EDC as a linker was employed to immobilize APBA onto the surface of AMNSs. Briefly, 0.22 M EDC and 0.22 M NHS were added to AMNSs (1 mL) and ultrasonicated for 30 min. After magnetic separation to remove EDC and NHS, AMNSs were dispersed in water followed by the addition of ethanol (2 mL) containing 450 mg APBA. After stirring for 3 h, the resulting mixture was separated using a magnet, washed three times with deionized water, and finally dispersed in water (20 mL) to obtain APBA modified AMNSs (APBA/AMNSs).

Characterization of lipid bilayer

Laser scanning confocal fluorescence microscopy

pAPG was dissolved in HEPES buffer (50 mM, pH 9.4) with different concentrations. 20 μL of pAPG and 5 μL of 2 mg/mL APBA/AMNSs solution were mixed, and the resulting mixture was

incubated with gentle shaking and then washed with HEPES buffer three time after 40 min, to

obtain pAPG/APBA/AMNSs. After that, 20 μL of DSPE-PEG-NHS (500 μM) in 20 mM HEPES

buffer (100 mM NaCl, 5 mM CaCl$_2$, pH 7.4) was added into the tube. Then the mixture was

washed three times with corresponding buffer after 50 min. Subsequently, 40 μL of Dio in DMSO

was dropped into the mixture with the desired molar ratios (DSPE-PEG-NHS : Dio = 99.5 : 0.5)

and washed five times after 30 min. Afterwards, 40 μL of cyanine 3 amine in 20 mM HEPES

buffer was mixed into the tube and incubated for 4 h. Finally, the mixture was washed by

corresponding buffer three times, and dissolved into 40 μL HEPES buffer for imagination.

Confocal fluorescence imaging was performed with a LSM710 laser scanning microscope (Occult

International Ltd, Germany) with a 20 × lens.

Fluorescence spectroscopy

The sample was prepared using the above method described in 1.2.1. Fluorescence spectra were

obtained using an F-7000 fluorescence spectrometer (Hitachi, Ltd., Japan). The emission spectra

were measured in the range from 450 nm to 600 nm and 500 nm to 650 nm with excitation

wavelengths of 484 nm and 555 nm for Dio and cyanine 3 amine, respectively.

Dynamic light scattering

The hydrodynamic sizes of the nanospheres at the different modified stages were tested by using

dynamic light scattering (DLS) instrument with a commercial Zetasizer (Malvern Instruments,

UK). The samples dissolved in 20 mM HEPES were firstly loaded into disposable cells and the

particle sizes were tested in triplicate at 25 $^{\circ}$C with 1.33 for refractive index of the dispersant. For

zeta potential measurements, samples were loaded in regular disposable cells and measurements

were performed using a dip probe.

Fourier transform infrared (FT-IR) spectrometer

FT-IR spectra were obtained on an VERTEX 70 Fourier Transform Infrared spectrometer (Bruker Co. Ltd., Bergisch Gladbach, Germany) fitted with deuterated triglycine sulphate detector. The spectra were recorded in transmission mode from 4000 cm^{-1} to 400 cm^{-1} at a resolution of 0.2 cm^{-1} at room temperature. All the scanned spectra were baseline-corrected using OPUS/IR analytical software.

Cell culture

Caco-2 cells were maintained in DMEM medium containing 10% fetal bovine serum and grown at 37 °C in a humidified incubator (5% CO_2 - 95% air). Those cells were harvested at the end of the log phase for the following experiments. After washing three times using warm PBS, cells were detached with 0.25% (w/v) trypsin and concentrated by centrifugation at 1000 $\times g$ for 5 min. The obtained cells were dispersed in sterile PBS buffer (pH 7.4) and then concentrated by centrifugation. Finally, the cells were re-suspended in PBS buffer. The number of cells was determined by hemocytometer counting (TC10™, Bio-Rad, USA).

Specificity analysis

150 μM BSA, Ova, ALP, LF, GHb, α-amylase, lipase, trypsin, and glucose oxidase were used to test the specificity of the established method. Meanwhile, 150 μM BSA, 150 μM Ova, 150 μM ALP, 150 μM LF, 150 μM GHb, 1.5 mM gallic acid, 15 μM quercetin, and 15 μM maltopentaose were separately mixed with 15 μM pAPG to investigate the specificity of enzyme substrate as a linker.

Results and discussion
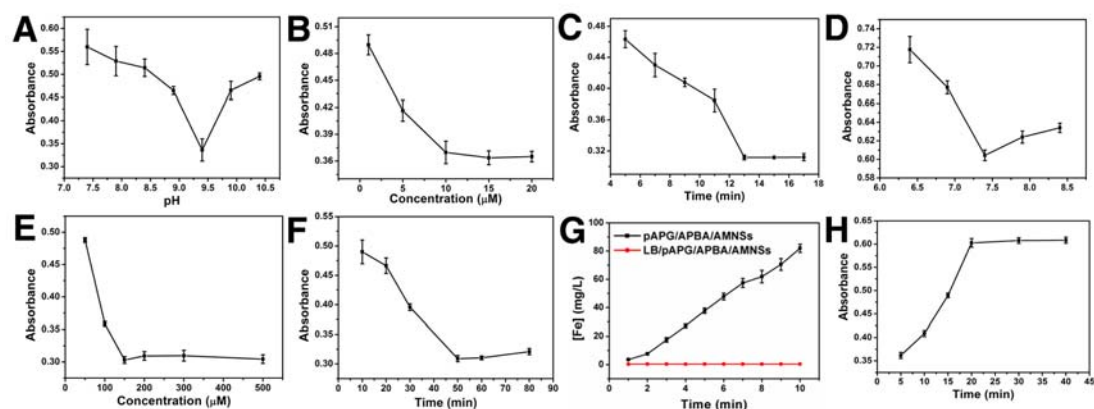
Optimization of experimental conditions

Figure S1. (A) The absorbance values versus pH values for pAPG binding with APBA/AMNSs. **(B)** The absorbance values versus pAPG concentrations. **(C)** The absorbance values versus the time for pAPG binding with APBA/AMNSs. **(D)** Absorbance values versus pH values for reaction between pAPG and DSPE-PEG-NHS. **(E)** Absorbance values versus concentration of DSPE-PEG-NHS. **(F)** Absorbance values versus time for reaction between pAPG and DSPE-PEG-NHS. **(G)** Iron ion concentrations versus leaching time for pAPG/APBA/AMNSs and LB/pAPG/APBA/AMNSs. **(H)** Absorbance values versus time for enzyme hydrolysis.

The pH value is an important parameter to determine the extent of pAPG binding with APBA/AMNSs. The lowest absorbance values can be observed with 9.4 of pH value (**Figure S1A**), signifying the maximum amount of pAPG coordinating with boronic groups located at the outer layer of APBA/AMNSs. So 9.4 is chosen as optimum pH value. The amount of boronic acid at the outer layer of APBA/AMNSs decides the binding number of pAPG molecules. As exhibited in **Figure S1B**, the absorbance values firstly decrease and then keep unchanged along with the increasing concentrations of pAPG from 0 μM to 20 μM. It suggests that boronic acid groups have

5

totally coordinated with 15 μM of pAPG. Therefore, 15 μM is chosen as optimum concentration for pAPG binding with APBA/AMNSs. The time has a clear influence on the efficiency of pAPG binding with APBA/AMNSs. As shown in **Figure S1C**, absorbance values remain unchanged when the binding time reaches 15 min, implying efficient coordination of pAPG with boronic acid units. Hence, 15 min is used as binding time. In order to achieve efficient reaction between pAPG and DSPE-PEG-NHS and enhance the efficiency of analytical method, the reactive pH value is optimized. The absorbance value minimizes at pH 7.4 (**Figure S1D**), suggesting the most efficient linkage of DSPE-PEG-NHS with pAPG/APBA/AMNSs. The result is in accordance with the previous report that the reaction between primary amine and NHS ester can be efficiently carried out at neutral pH value [2]. In addition to pH value, the concentration of DSPE-PEG-NHS and time also influence the reaction efficiency between primary amine of pAPG and NHS ester. As shown in **Figure S1E**, the absorbance values almost keep unchanged when the concentration of DSPE-PEG-NHS increases to 150 μM, signifying the total covering of MNSs by DSPE-PEG-NHS. Meanwhile, the reaction can fully proceed within 50 min (**Figure S1F**). Accordingly, 150 μM and 50 min are separately used as the optimal concentration of DSPE-PEG-NHS and time for pAPG reacting with DSPE-PEG-NHS. The amount of iron ion has an obvious influence on the oxidation degree of ABTS and the performance of the established method, so iron ion release kinetic process has been investigated. Along with the prolonged time, the concentrations of the released iron ion increase for pAPG/APBA/AMNSs (blank curve, **Figure 1G**). On contrary, almost no iron ion are released from LB/pAPG/APBA/AMNSs with 15 μM pAPG (red curve, **Figure 1G**). Considering the credible absorbance range and the efficiency of the method, 5 min is selected as the leaching time for the release of iron ion. We further study enzyme reaction kinetics and the corresponding

results are shown in **Figure S1H**. With the increase of hydrolysis time from 5 min to 40 min, the absorbance values gradually rise and subsequently remain unchanged. In the presence of α-Glu, pAPG is converted into pAP and α-glucose [3], resulting in the happening of α-glucose/APBA/AMNSs after magnetic separation. The composite can not link with DSPE-PEG-NHS, leading to no occurrence of lipid bilayer around AMNSs and the corresponding increase of absorbance values. The absorbance values keep unchanged after 20 min, implying the completely hydrolysis of pAPG. Consequently, 20 min is used as optimal time for enzyme hydrolysis reaction.
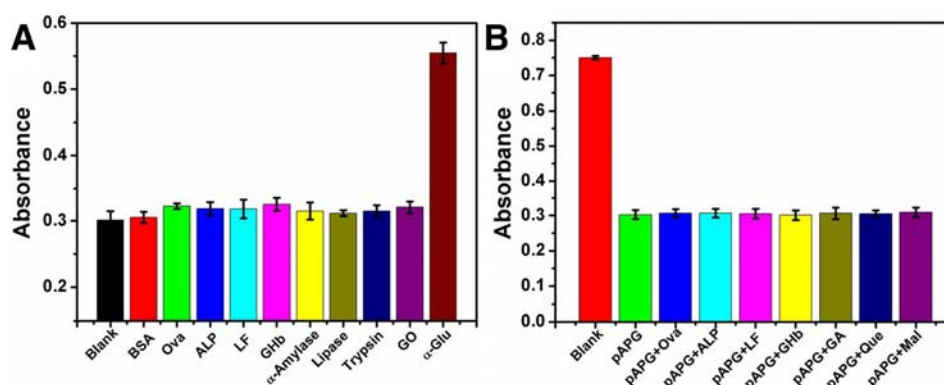
Specific analysis

Figure S2. (A) Specific investigation of the established method using BSA (500 μg/mL), Ova (500 μg/mL), ALP (20 U/mL), LF (500 μg/mL), GHb (500 μg/mL), α-amylase (20 U/mL), lipase (20 U/mL), trypsin (20 U/mL), and GO (20 U/mL) instead of α-Glu (1 U/mL). **(B)** Specific analysis of enzyme substrate as a linker using blank, pAPG (15 μM), pAPG + Ova (150 μM), pAPG + ALP (150 μM), pAPG + LF (150 μM), pAPG + GHb (150 μM), pAPG + GA (1.5 mM), pAPG + Que (15 μM), pAPG + Mal (15 μM) instead of pAPG (15 μM).

In order to investigate the specificity of the established method, the substances including pure

protein (BSA), glycoproteins (Ova, ALP, LF, and GHb), and enzymes (α-amylase, lipase, trypsin, and GO) have been chosen instead of α-Glu, and the experimental results are shown in **Figure S2A**. Low absorbance values can be obtained for these interference components with more than 20 time concentration higher than that of α-Glu, which can be ascribed for the shortage of their specific catalyzed ability for cleavage of pAPG. On the contrary, high absorbance value can be observed in the presence of α-Glu, signifying the existence of numerous iron ions in the solution. Due to specific catalyzed capability of α-Glu on the hydrolysis of pAPG into pAP and α-glucose, the number of pAPG will decrease, resulting in the declined assembly of lipid bilayer and the corresponding weak inhibition effect on the transport of iron ions.

Furthermore, the favorable coordination of pAPG with APBA/AMNSs is vital for the establishment of detection method for α-Glu activity and its inhibitor analysis. To inspect the competent binding capability of pAPG, glycoproteins (Ova, ALP, LF, and GHb) containing diols groups and primary amino groups, and the inhibitors (GA, Que, and Mal) with diol group have been chosen and the results are given in **Figure S2B**. The mixtures of pAPG and different glycoproteins with 10 time concentrations higher than that of pAPG, exhibit low absorbance values. It suggests that glycoproteins have no obvious effect on the binding of pAPG, as a result of their high molecular weight restricting the binding velocity. For GA, Que, and Mal, the concentrations with the maximized inhibition efficiency are used. Similar to that of pAPG, the mixtures of pAPG and various inhibitors also show low absorbance values, indicating the negligible influences of these substances on the coordination of pAPG. In comparison with diol groups of phenyl ring moieties in the structures of GA and Que, *cis* 2'-OH and 4'-OH of saccharide moiety of pAPG owns stronger coordination ability with boronic acid on the surface of

8

APBA/AMNSs [4]. For Mal, its inferior binding can be explained for relative high molecular weight compared to that of pAPG.

Overall, these results well confirm the good selectivity and specificity of our established colorimetric method for the analysis of α-Glu activity and its inhibitors.
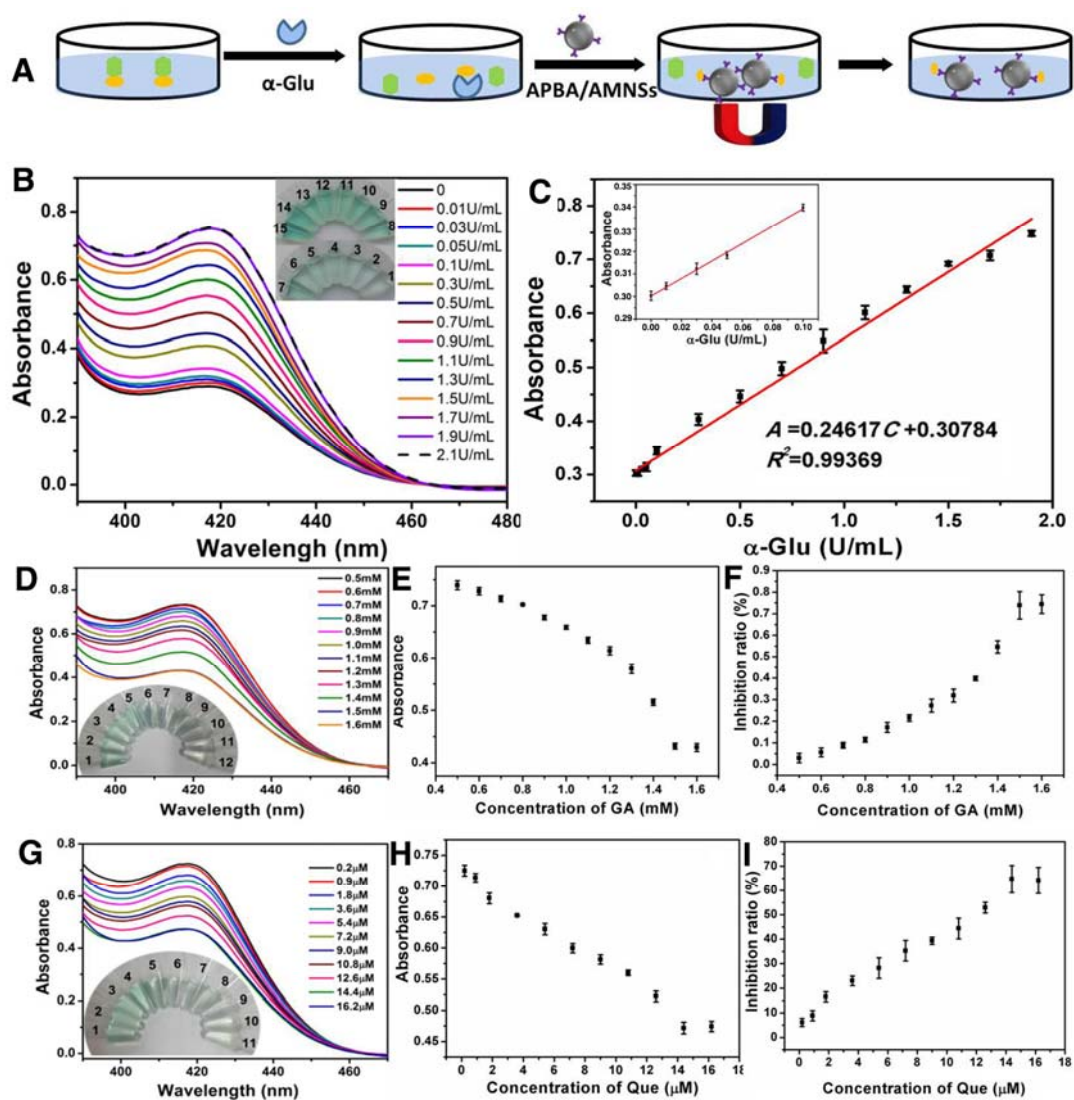
Purified α-Glu assay and its inhibitor screening

Figure S3. (A) Schematic illustration for capture of enzymatic hydrolyzed product through magnetic separation. **(B)** UV-vis spectra and photographs (inset) of the mixtures prepared by the addition of various concentrations of enzyme. Inset, from vial 1 to vial 15: the enzyme concentrations are 0, 0.01, 0.03, 0.05, 0.1, 0.3, 0.5, 0.7, 0.9, 1.1, 1.3, 1.5, 1.7, 1.9, and 2.1 U/mL.

(C) Linear calibration curve corresponding to absorbance values against enzyme concentrations. Inset: the magnified calibration curve. **(D)** UV-vis spectra and photographs (inset) of the solution, **(E)** Absorbance values, and **(F)** Inhibition ratios upon analyzing various concentrations of GA. Inset (E), vial 1 to vial 9: GA concentrations were 0.5, 0.6, 0.7, 0.8, 0.9, 1, 1.1, 1.2, 1.3, 1.4, 1.5, and 1.6 mM. **(G)** UV-vis spectra and photographs (inset) of the solution, **(H)** Absorbance values, and **(I)** Inhibition ratios upon analyzing various concentrations of Que. Inset (G), vial 1 to vial 9: Que concentrations were 0.2, 0.9, 1.8, 3.6, 5.4, 7.2, 9, 10.8, 12.6, 14.4, and 16.2 μM. Error bars indicate standard deviations (n = 3).

In the assay, the self-assembled lipid bilayer has been firstly proposed and its inhibition on ion transport is utilized for enzyme activity analysis. The absorption spectra upon analyzing different concentrations of α-Glu are shown in **Figure S3B**. With the increase of α-Glu concentrations from 0 U/mL to 2.1 U/mL, the color of the solution gradually turns from colorless to dark green (from vial 1 to vial 15, inset in **Figure S3B**) and a progressively increase occurs in the UV-vis spectra (**Figure S3B**). In the presence of α-Glu, pAPG can be converted into pAP and glucose. APBA/AMNSs can coordinate with glucose to give glucose/APBA/AMNSs. After magnetic separation, pAP and enzyme are removed from the solution (**Figure S3A**). The two products have no capability for the linkage of DSPE-PEG-NHS onto APBA/AMNSs, leading to no occurrence of self-assembly of lipid bilayer around AMNSs and the subsequent leaking of iron ions into the solution and correspondingly strong ABTS oxidation.

The absorbance values have been used for the quantitative detection of α-Glu. As depicted in **Figure S3C**, the absorbance values linearly increase with the increasing enzyme concentrations

from 0.01 U/mL to 1.9 U/mL, which is wider than the previous reports [5, 6]. Meanwhile, the regression equation of $A = 0.24617\ C + 0.30784$ ($R^2 = 0.99369$) is given. In addition, by the interpolation of the mean plus three times the standard deviation of the zero standards, the detection limit has been calculated to be 0.0016 U/mL, low than the values reported previously [6]. For α-Glu assay, the colorimetric measurements have been proceeded for at least three times independently. The detection precision has been investigated using the slope of the regression of enzyme (from 0.01 U/mL to 1.9 U/mL) and the RSD value of the three slopes is 1.83%, which indicates acceptable precision and reproducibility of the current established method.

It is reported that α-Glu inhibitors are especially well-suited to treat postprandial hyperglycemia, a common and serious problem faced by many people with Type 2 diabetes [7]. In order to test the practicability of the developed method to analyze the α-Glu inhibitor, two compounds with different inhibition mechanism have been chosen as model compounds.

As a kind of competitive inhibitor, GA can competitively bind the active site of the enzyme [8] so as to hinder the cleavage of glycosidic bond in the pAPG and decrease the oxidized extent of ABTS catalyzed by iron ions released from APBA/AMNSs in the acid solution. With the increase of GA concentrations from 0.5 mM to 1.6 mM, the color of the solution gradually changes from dark green to colorless (vial 1 to vial 12, inset in **Figure S3D**) and a decrease happens in the UV-vis spectra (**Figure S3D**). As exhibited in **Figure S3E**, the absorbance values decline with the rising GA concentrations and then keep unchanged, suggesting a dose-dependent manner for the inhibition of GA on enzyme activity. Meanwhile, the inhibitory ratios gradually increase and then level off along with the increasing GA concentrations (**Figure S3F**). It is found that 1.5 mM GA can evidently inhibit enzyme activity since no clearly change in either spectra or the solution color

(**Figure S3D**). A maximum inhibitory ratio of 80.25% with IC_{50} value of 1.4 mM can be obtained

for GA, in accordance with the previous report [9].

Different from GA, Que can inhibit α-Glu activity noncompetitively and anticompetitively [10].

The unsaturated C ring, 3-OH, 4-CO, and hydroxyl substitution on the B ring are vital groups and

both the 3'-OH and 4'-OH groups can interact with amino acids Asp 214 and Glu 276 of enzyme

active group to prevent the cleavage of glycosidic bond for inhibition effect of Que [11]. As shown

in **Figure S3G**, along with the increase of Que concentrations from 0.2 μM to 16.2 μM, solution

color turns from dark green to colorless (vial 1 to vial 11, inset in **Figure S3G**), consistent with the

observed change of absorbance values in the spectra (**Figure S3H**). The absorbance value remains

unchanged once the Que concentration attains to 14.4 μM (**Figure S3H**). The maximum inhibition

ratio of Que is 70.99%, with IC_{50} value of 13.5 μM (**Figure S3I**), in well agreement with the

values in the previous report [10].

References:

[1] Lu AH, Salabas EeL, Schüth F. Magnetic nanoparticles: synthesis, protection, functionalization,

and application. Angew Chem Int Edit. 2007; 46: 1222-44.

[2] Hermanson GT. Bioconjugate techniques: London, UK: Academic Press; 2013.

[3] Zhang J, Liu Y, Wang X, Chen Y, Li G. Electrochemical assay of α-glucosidase activity and the

inhibitor screening in cell medium. Biosens Bioelectron. 2015; 74: 666-72.

[4] Xia N, Zhang L, Feng Q, Deng D, Sun X, Liu L. Amplified voltammetric detection of

tyrosinase and its activity with dopamine-gold nanoparticles as redox probes. Int J Electrochem

Sci. 2013; 8: 5487-95.

[5] Chen H, Zhang J, Wu H, Koh K, Yin Y. Sensitive colorimetric assays for α-glucosidase activity and inhibitor screening based on unmodified gold nanoparticles. Anal Chim Acta. 2015; 875: 92-8.

[6] Zhang J, Liu Y, Lv J, Li G. A colorimetric method for α-glucosidase activity assay and its inhibitor screening based on aggregation of gold nanoparticles induced by specific recognition between phenylenediboronic acid and 4-aminophenyl-α-d-glucopyranoside. Nano Res. 2015; 8: 920-30.

[7] Ag H. Pharmacology of α-glucosidase inhibition. Eur J Clin Invest. 1994; 24: 3-10.

[8] Wan C, Yuan T, Li L, Kandhi V, Cech NB, Xie M, et al. Maplexins, new α-glucosidase inhibitors from red maple (Acer rubrum) stems. Bioorg Med Chem Lett. 2012; 22: 597-600.

[9] Cirillo G, Kraemer K, Fuessel S, Puoci F, Curcio M, Spizzirri UG, et al. Biological activity of a gallic acid-gelatin conjugate. Biomacromolecules. 2010; 11: 3309-15.

[10] Li YQ, Zhou FC, Gao F, Bian JS, Shan F. Comparative evaluation of quercetin, isoquercetin and rutin as inhibitors of α-glucosidase. J Agr Food Chem. 2009; 57: 11463-8.

[11] Phan MAT, Wang J, Tang J, Lee YZ, Ng K. Evaluation of α-glucosidase inhibition potential of some flavonoids from Epimedium brevicornum. LWT-Food Sci Technol. 2013; 53: 492-8.